Karaj branch

Journal of Applied Chemical Research
jacr.kiau.ac.ir

Journal of Applied Chemical Research, 12, 1, 79-91 (20187)

Study on Sunitinib Adsorption on Graphene Surface as an Anticancer Drug

Sepideh Tanreh[1], Abolghasem Shameli[2*], Ebrahim Balali[1]

[1]Department of Chemistry, Pharmaceutical Sciences Branch, Islamic Azad University, Tehran, Iran

[2]Department of Chemistry, Faculty of Science, Omidiyeh Branch, Islamic Azad University, Omidiyeh, Iran*

(Received 14 Mar. 2017; Final version received 12 Jun. 2017)

Abstract

In recent years, Nano technology and its application have moved to discovering chemical therapy drugs. Research, development for finding new targets in tumors, targeting methods and stabilizing the nano particle in targeted cells is based on drug delivery and its crucial effect. Examining the computational controlled drug delivery by graphene sheets has become very significant due to numerous side effects of this drug especially on nervous system as a result of direct injection. In this work, adsorption of Sunitinib on Si and Al or nitrogen doped graphene has been studied using density functional theory. Doping Si or Al significantly affects the adsorption of Sunitinib over graphenes. Still, not much impact of doping Ni on graphene is observed. Interaction energy, estimated using the super molecular approach ranges from 54.97 KJ mol^{-1} to 63.95 KJ mol^{-1} in the gas phase. Furthermore, the calculated density of states (DOS) shows the existing of noteworthy orbital hybridization between Sunitinib and Si or Al doped graphene during the adsorption process which is trying out to strong interaction while there is no evidence for hybridization between the those molecules and the pristine graphene. ^{11}C and ^{1}H chemical shielding correlate noticeably with the derivatives graphene. ^{11}C, ^{27}Al and ^{2}H nuclear quadrupole coupling constants, C_Q, and asymmetry parameter, η, reveal the remarkable effect of Sunitinib adsorption on electronic structure of the graphene.

Keywords: *Graphene, Binding energy, Chemical shielding, Nuclear Magnetic Resonance, Nuclear Quadrupole Resonance, Density Functional Theory.*

[*]***Correspond author:*** *Abolghasem Shameli, Department of Chemistry, Faculty of Science, Omidiyeh Branch, Islamic Azad University, Omidiyeh, Iran. E-mail: shameli678@gmail.com.*

Introduction

Drug delivery systems have been created for improving therapeutic properties of the drugs and are often in form of a drug-containing capsule. Such systems releases the drugs at specific amount in a specific site, therefore they affect drugs' pharmacokinetics and distribution. Nanoparticles have been widely applied in drug delivery. Recently, nanostructures' fabrication as drug-carriers has drawn considerable attention. These structures- due to slow drug release, drug molecule protection, having sizes smaller than a cell, capability of passing biological barriers, enhancement of drug durability in blood, targeted drug delivery and biocompatibility- can be regarded as effective drug delivery systems which result in enhancement of therapeutic efficiency of the drug. During last decades, advancement in different disciplines, namely polymer science, chemistry, biology, mechanics and physics, affected the diversity of nano-carriers and introduced various classes of carriers with unique properties and different application to the medicine [1]. Fast development of nanotechnology for disease diagnosis and treatment has occurred. Fullerene nanoparticles and their deviants can overcome to resistivity of some diseases against specific drugs and hence used as nano drug-carrier [2-5].

Due to its unique properties such as high thermal conductivity, electron transport, high mechanical strength, having vast surface for bi-lateral adsorption in 2 dimensions, Graphene is one of the most important nanostructures. Experimental and theoretical analyses on adsorption of molecules such as Li, NH_2, NO_2, H_2O, CO_2, CO, O_2, amino acids and DNA on graphene, revealed stable adsorption of these molecules on graphene [6-7]. Extensive surface of graphene is one of the reasons providing various applications for that. Many reports revealed low toxicity of graphene and its derivatives for drug delivery purposes. Graphene oxide is superior on graphene in terms of having hydrophilic functional groups. Slight toxicity of graphene could be resolved by its surface functionalization via polymer and other nanoparticle [8].

Boron Nitride nanotube has attracted significant attention due to its special mechanical properties, chemical and thermal stability, electrical properties and more importantly its high biocompatibility. Many researches proved that these nanotubes have high biocompatibility and have the ability to interact with organic molecules such as protein and DNA [9-11]. They are not toxic for cells and do not damage DNA [12]. These properties have made them a proper nano-carriers for medical purposes as alternatives to CNTs [13]. Their functionalization with various molecules, have given them unique properties as smart and

targeted carriers for medical purposes especially cancer therapy. Functionalization is realized by weak physical forces or covalent chemical bonds [14-15]. This study investigated structural, electronic and chemical stability of graphene nano-sheets and Al, Ga, N and P-doped graphene complexes with sunitinib drug via DFT tools. These complexes can be appropriate nano-carrier for anti-cancer drug of Sunitinib.

Sunitinib, with commercial name of Sutent, is an anti-cancer drug and multi-kinase inhibitor preventing growth and development of cancerous cell. It has been used for treatment of specific types of advanced stomach, intestine, gastrointestinal tract, pancreas, kidney or esophageal tumors [16-21]. This drug can damage fetus or cause impairments at the time of birth, it can also pass from mother milk and harm the child. Sunitinib can cause intensive or fatal effects in liver and results in many liver problems such as Nausea, upper stomach pain, itching, fatigue, loss of appetite, dark urine, clay-colored stools, and jaundice (yellowing of the skin or eyes).

In recent years, 19-21 differently functionalized carbon nanotubes and graphene have been used in cancer therapy as a molecular carrier or drug delivery. Flourcine and β-amphotreicine cab successfully attach to functionalized CNTs for their transport to mammalian cells without losing their anti-fungi properties. In a similar method, an anti-cancer drug such as Metoterxate was attached to a multi-walled CNT for its transport to the selected cell [23]. Multi-walled CNTs and graphene oxide were functionalized with PVA [24]. For Camtotcine loading, the anti-cancer drug was employed via π-π interaction and its transport for treatment of breast and skin cancer. Chen et al. [25] observed that CNTs are inherently non-toxic and could be functionalized for protein and cell attachment. Regarding higher need of cancerous cells to folate, boron nitride nanotubes can be functionalized with folate. Such sort of nanotubes would be considerably absorbed by tumors an act as smart carriers in cancertherapy [26].

Folate-functionalized boron nitride nanotubes act as boron transporter in malignant multiform Glioblastoma cells. This can be employed as effective boron target for boron neutron trapping treatment in malignant brain tumors, while the functiolized groups act as inhibitors for other peptides or proteins via biological functions. The effect of boron nitride nanotubes functionalized with porous silica nanoparticles for Dexor and Bicine anti-cancer drug delivery to prostate cancerous cells was investigated. It was observed that these nanotubes have higher ability for killing cancerous cells in comparison with pristine nanotubes which

could be attributed to high drug loading and also controlled release of drug due to silica pores [27]. Theoretical studies on covalent and non-covalent interactions of boron nitride nanotubes with biomolecules have resulted in stability and electronic properties' discovery about the molecule for their employment as drug carriers. DFT and molecular dynamic simulations exhibited the potential of boron nitride nanotubes for encapsulation of anti-cancer molecules such as carbo-platinum for delivery to target cells [28]. DFT calculations of plain wave pseudopotentials [29] were conducted for investigating the interaction between boron nitride nanotubes and three amino acids with different polarities. In similar studies [30] it was observed that amino acids and n-sites surrounded in nanotube cavity have only weak interactions which can be used as channels for biomolecule transport.

Experimental

We have performed density functional theory (DFT) calculations to optimize the structural models of Sunitinib(Sun) and the representative. A hexagonal graphene (Gr) supercell (5 × 5 graphene unit cell) containing 72 carbon atoms was chosen as the basic model for the calculations. The Si- and Al- graphene were then modeled by substituting a single Si or Al atom for one C atom on the surface. Interaction of Sunitinib molecule with the graphene systems has been studied in the gas. This reduces the computational cost in comparison to treating each molecule separately. All the structures were optimized at 6-311G* level of theory. The B3LYP exchange-correlation functional and the 6-311G standard basis set have been used to run all computations as implemented in the Gaussian 03 package [31]. It has been found that the NMR parameters calculated by B3LYP levels are in good agreement. The adsorption energy of the adsorbate Sunitinib with the doping graphene is calculated according to the formula:

$$\Delta E_{ads} = E_{Sun\text{-}Gr} - (E_{Gr} + E_{Sun}) \qquad (1)$$

where $E_{Gr\text{-}Sun}$, E_{Sun} and E_{Gr} are the total energies of the adsorbate–substrate (Gr-Sun) system, the substrate (Sun), and adsorbate (Gr), respectively. Analysis was performed at the B3LYp/6-311G* level. The molecular systems include the individual graphene, the individual Sun, and hybrid Gr-Sun (Figure 1).

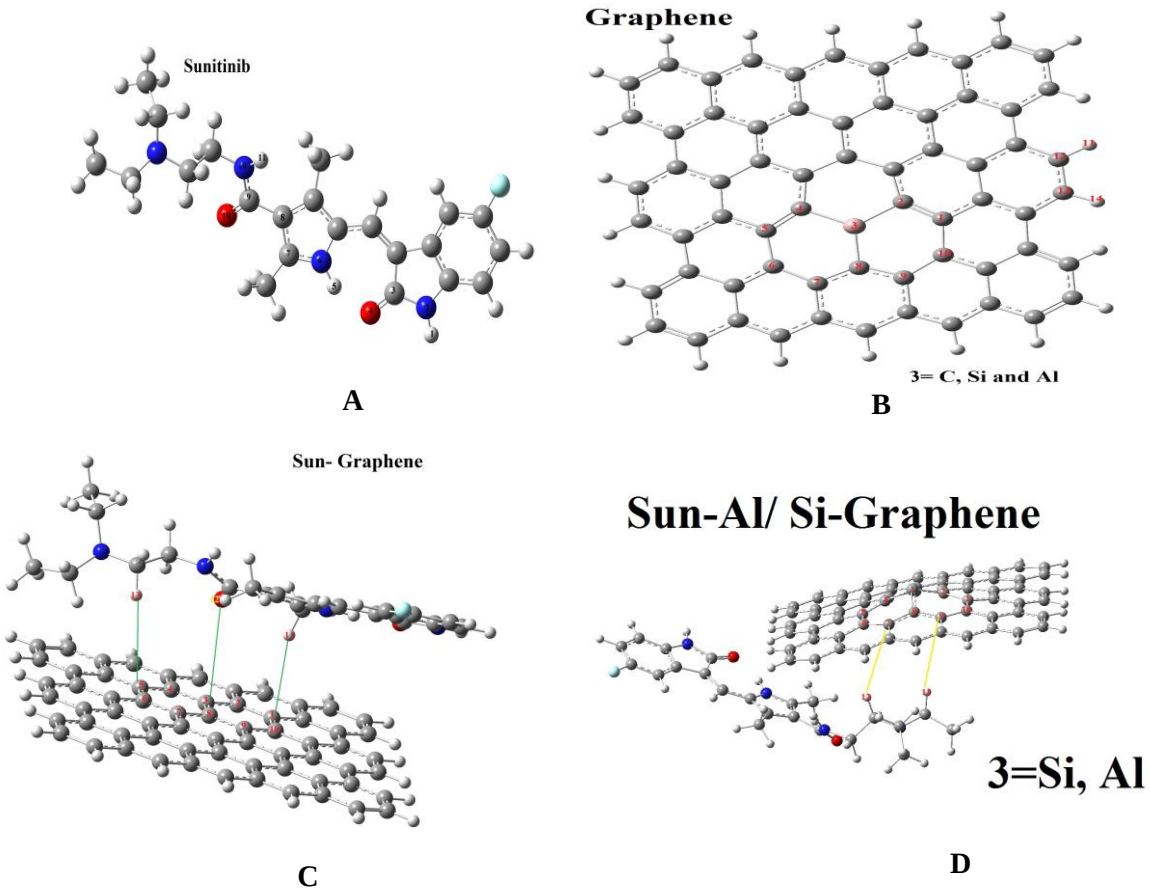

Figure 1. The optimized structure of structure a) Sunitinib b) graphene with dopeing Al and Si c) graphene with sunitinib d) Al and Si doped graphene.

Results and discussion

Optimized structures of Al and Si-graphene

At first, it is important to study the geometric structure and electronic properties of optimized Al- and Si-graphene sheets compared to the pure graphene. Figure 1 (model B) shows the geometric structure of the isolated Al- and Si-graphene sheets after the geometry optimization. Due to symmetry of electronic distributions in the original gr structures, the values of dipole moments (DM) of them are zero. However, variations of these symmetric situations in the doping Al/Si models increase the magnitudes of dipole moments. Different magnitudes of energies for HOMO and LUMO levels are observed for the gr and doping models. The magnitudes of energy gaps (E_{gap}), which show the energy differences between HOMO and LUMO levels, are slightly decreased for the Al/ Si structures in comparison to their corresponding gr structures. However, the magnitudes of E_{gr} for Al/Si structures are equal to the magnitudes of corresponding Al/Si structures, implying the role of Al/ Si in the

electronic conductivity of graphene. Moreover, the energy differences between HOMO and LUMO levels are decreased for pristine graphene (Table 1).

Table 1. Optimized properties for the model B, C and D.

Atoms (length bond (A^0)	Gr	Al-gr	Si-gr	Atoms (length bond (A^0)	Sun-gr	Sun-Al-gr	Sun-Si-gr
H11-C12	1.08	1.08	1.08	C1-C2	1.42	1.40	1.41
C12-C13	1.38	1.39	1.39	C2-X3	1.43	1.83	1.75
C13-H14	1.08	1.09	1.08	X-C4	1.44	1.83	1.75
C1-C2	1.42	1.37	1.40	C4-C5	1.42	1.40	1.41
C2-X3	1.43	1.75	1.68	C5-C6	1.43	1.47	1.47
X3-C4	1.43	1.75	1.68	C6-C7	1.43	1.45	1.45
C4-C5	1.42	1.37	1.40	C7-C8	1.43	1.40	1.42
C5-C6	1.44	1.52	1.48	C8-C9	1.42	1.40	1.42
C6-C7	1.41	1.49	1.46	C8-X3	1.44	1.83	1.75
C7-C8	1.42	1.39	1.41	C9-C10	1.42	1.45	1.45
C8-C9	1.42	1.39	1.41	C10-C1	1.43	1.48	1.47
C8-X3	1.43	1.75	1.69	C4or7-H12	3.26	2.97	3.83
C10-C1	1.44	1.52	1.48	C2 or 9-H11	3.55	3.63	3.86
DM (Debye)	0.0001	1.0905	0.3157	-	2.31	2.82	2.77
E_{HOMO} (ev)	-0.13673	-0.16	-0.13605	-	-0.280	-0.304	-0.139
E_{LUMO} (ev)	-0.12534	-0.11	-0.12456	-	-0.277	-0.271	-0.127
E_{gap} (kj/mol)	-0.0114	-0.0547	-0.0115	-	-0.288	-3.237	-1.102
E_{Ads} (kj/mol)	-	-	-	-	-63.95	57.98	-54.97
E (kev)	-68.81	-74.36	-75.64	-	-104.83	-109.79	-111.67

**DM= dipole moment*

As can be seen in Figure 1(model B), the geometric structure of graphene changes significantly after doping of the graphene sheet by the Al atom,. The larger bond lengths combined with the different bond angles force Al to protrude from the sheet as well as to displace the positions of the first and second neighbors out of the plane. The average bond length between the central C (Al) atom and the adjacent C atoms are elongated from 1.74 Å in the pristine graphene to 1.42 Å in Al-graphene, along with the distortion of hexagonal structure of the graphene sheet. In the case of Si-graphene (Figure 1), the Si dopant with a larger atomic radius than Al atom is pushed outside the graphene plane and this leads to the average elongation of three newly formed Si–C bonds (1.68 Å) compared to the C–C bond of the pristine graphene.

Sunitinib adsorption over Al- and Si-doped graphene

According to Figure 1, the bond lengths of Al and Si dopants to carbon are increased due to the Sun adsorption on the graphene surface. Since the bond angle is reduced by about 109^o, Al and Si disturbance is changed from sp^2 to sp^3 hybrid. Hence, the bond length of Al-C and

Si-C are changed to 1.84 A^o and 1.75 A^o, respectively. The adsorption energy of Sun-Gr is -6394872.95 KJ/mol. Considering the adsorption energy, it can be found that the nano-drug of Sun-Al-Gr has the maximum adsorption. Since the adsorbed energy is more than 8 J/mol, then the adsorption is a chemical interaction where a strong Van der waals force exists between the drug and graphene and the London force of Al-Sun-Gr is the strongest. The bipolar moment of the graphene is increased due to the adsorbed Sun on the graphene surface. Then it can be concluded that the solubility of the nano drug (Sun-Gr) is increased and it probably can play the role of drug delivery inside the body (Ttable 1).

Nuclear Quadrupole Resonance

Nuclear Quadrupole Resonance (NQR) is one of the promising chemical techniques for identifying the composite of the elements which collaborates with nuclear magnetic resonance. Unlike NMR, the NQR analysis can be detected even in the absence of magnetic field in nuclear conversion. In simpler terms, the NQR spectroscopy functions the same as NMR with zero magnetic field. In fact the NQR resonance is a connection between electric field gradient (EFG) and Nuclear quadrupole resonance in which the charge distribution takes place. The EFG, demonstrates the total transformation of an element, furthermore a location of a nuclei in material in which the linked valance electrons of the atoms which are altered is shown as well. Indeed, this frequency is in good agreement with nuclear quadrupole resonance, nuclei properties and EFG of neighbor nuclei in a composite or a crystal.

As well as the optimized properties, quadrupole coupling constants (C_Q) have been calculated for the atoms of optimized structures in order to distinguish the properties of investigated models at the atomic levels (Table 2). Electric field gradient (EFG) tensors have been evaluated as well and they have been changed into C_Q parameters using equation C_Q (MHz) = $e^2Qq_{zz}h^{-1}$, in which e, Q, q_{zz}, and h respectively stand for electronic charge, nuclear electric quadrupole moment, EFG tensors main eigen value, and Planck's constant [10]. Due to sensitivity of EFG tensors to electronic sites of atoms, they are able to reveal any perturbations employed to these sites demonstrating insightful information about the electronic features of matters [32]. The magnitudes of C_Q could be evaluated by means of nuclear quadrupole resonance (NQR) spectroscopy; furthermore they could take the advantage of being accurately reproduced through quantum computations by means of computational chemistry for predication and analysis of experimental investigations [33-35].

The standard Q values (Q (^{11}C)=33.27 mb, ^{17}O=-25.58 and ^{27}Al=146.6 mb) reported by Pyykkö [36].

Table 2. NQR parameters for Sun-gr, Sun-Al-gr and Sun-Si-gr.

atom	Sun-gr		atom	Sun-Al-gr		atom	Sun-Si-gr	
	η_Q	C_Q		η_Q	CQ		η_Q	C_Q
C9	0.00	1.75	C1	0.00	3.99	C1	0.00	3.99
C10	0.00	1.75	C2	0.00	3.99	C2	0.00	3.99
H11	0.00	0.00	C4	0.00	3.99	C4	0.00	3.99
			C7	0.00	3.99	C7	0.00	3.99
			C8	0.00	3.99	C8	0.00	3.99
			C9	0.00	3.99	C9	0.00	3.99
			C10	0.00	3.98	C10	0.00	3.98
			H11	0.00	0	H11	0.00	0
			H12	0.00	0	H12	0.00	0
			Al3	0.00	196.13	Si3	0.00	-
average	0.00	1.75		0.00	6.87		0.00	3.99

Mirzaeie and colleagues have reported the value of C_Q for graphen atoms (5,5) 1.7-2.3. The value has decreased as a result of attaching Sunitinib on graphen surface.In other words, the electric charge value is not along the z-z axis. By doping the central atom of graphene with Al and Si and attaching Sunitinib on its surface, the value of C_Q increases in all carbon atoms and the C_Q of Al atom changes to 196 which demonstrates the highest impact in comparison to pristine graphene.

Nuclear Magnetic Resonance

In this computational study, the properties of the electronic structure and chemical shielding parameters of the graphene were evaluated through density functional theory (DFT) calculations of the Nuclear Magnetic Resonance (NMR) parameters. The chemical shielding (C_S) tensors were calculated according to the gauge consist of atomic orbital (GIAO) approach [37]. The calculated C_S tensors in principal axis system (PAS) (d_{zz}> d_{yy}> d_{xx}) were converted to measurable NMR parameters, chemical shielding isotropic (C_{SI}) and chemical shielding anisotropic (C_{SA}) by using Eqs. (1) and (2), respectively [38]. The evaluated NMR parameters are exhibited in Table 3.

$$C_{SI}= 1/3(\sigma_{xx} + \sigma_{yy} + \sigma_{zz}) \qquad \text{Equation (1)}$$

$$C_{SA}= \sigma_{zz} - ½(\sigma_{yy} + \sigma_{xx}) \qquad \text{Equation (2)}$$

Table 3. Parmeters Nuclear Magnetic Resonance.

	Sun-Si-graphene				**Sun-Al-graphene**				**Sun--graphene**			
atoms	isotroic	Anystropy	C_{SI}	C_{SA}	isotroic	Anystropy	C_{SI}	C_{SA}	isotroic	Anystropy	C_{SI}	**C_{SA}**
C1	68.3	156.2	68.3	137.7	68.9	156.6	68.9	101.8	-	-		-
C2	67.8	183.4	67.8	146.4	67.8	180.8	67.8	107.1	-	-		-
C4	73.6	151.0	73.6	126.3	74.5	149.8	74.7	99.8	73.6	149.5	73.6	**60.7**
C7	71.8	152.0	71.8	67.6	72.8	152.2	72.8	51.2	71.5	152.2	71.5	**63.6**
C8	72.7	154.2	73.7	132.8	73.7	151.4	77.1	100.3	73.3	152.2	73.3	**60.8**
C9	71.8	152.0	71.8	115.1	72.6	151.0	72.6	113.9	73.4	149.5	73.4	**58.2**
C10	74.2	149.7	74.2	125.9	72.3	156.0	72.3	123.6	67.7	157.0	67.7	**60.7**
H11	30.0	8.1	30.0	6.8	31.1	9.7	31.1	8.0	-	-		-
H12	30.8	12.3	30.8	7.5	32.7	17.1	32.7	9.2	30.7	11.1	30.7	**1.4**
X=Al	-	-	-	-	325.8	162.2	325.8	103.2	--	-	-	-

In Table 3, the evaluated C_{SA} parameter for ^{11}C is 131.1-169.4 ppm and the maximum Anisotropic effect accounts for C 8 while for hydrogens in nano drug (Sunitinib-graphene) the C_{SA} is 1.4-3.5 ppm. In Sunitinib-graphene-Al C_{SA} for carbon atoms is 101.6-168.5 ppm in which the doping Al has caused C4 to be deshielded and C1,C9,C10 have the highest Anisotropic effect and become shielded. In nano drug (Sunitinib-graphene-Si) C_{SA} is 63.8-162.5 and C12,C10 has the highest value 162.5 and 156, respectively.

HOMO and LUMO parameters and density of state (DOS)

In Figure 2, the electronic density of states (DOS) of individual derivatives graphene were presented. The figures indicate the molecular orbitals of each element per to hole system that calculated using the Gaussview software. HOMO and LUMO energies and the corresponding energy gap (E_{gap} in ev) are two main parameters which are used for characterizing the electronic properties of graphene derivatives.

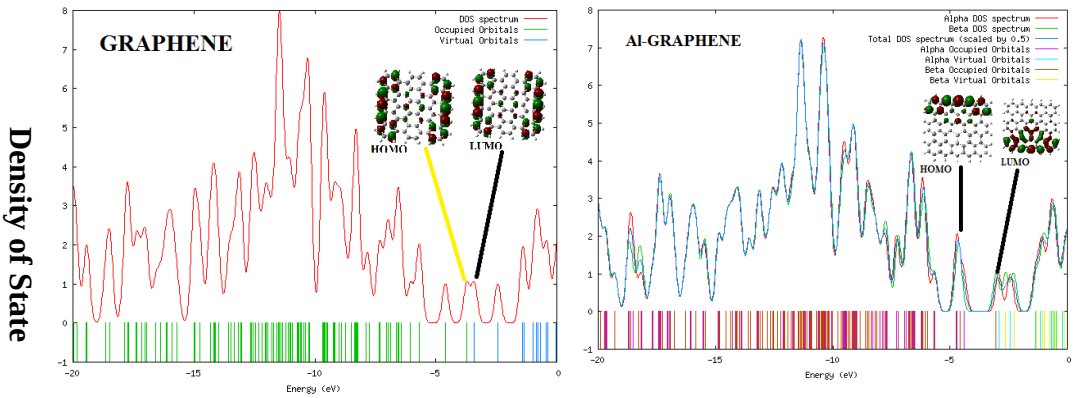

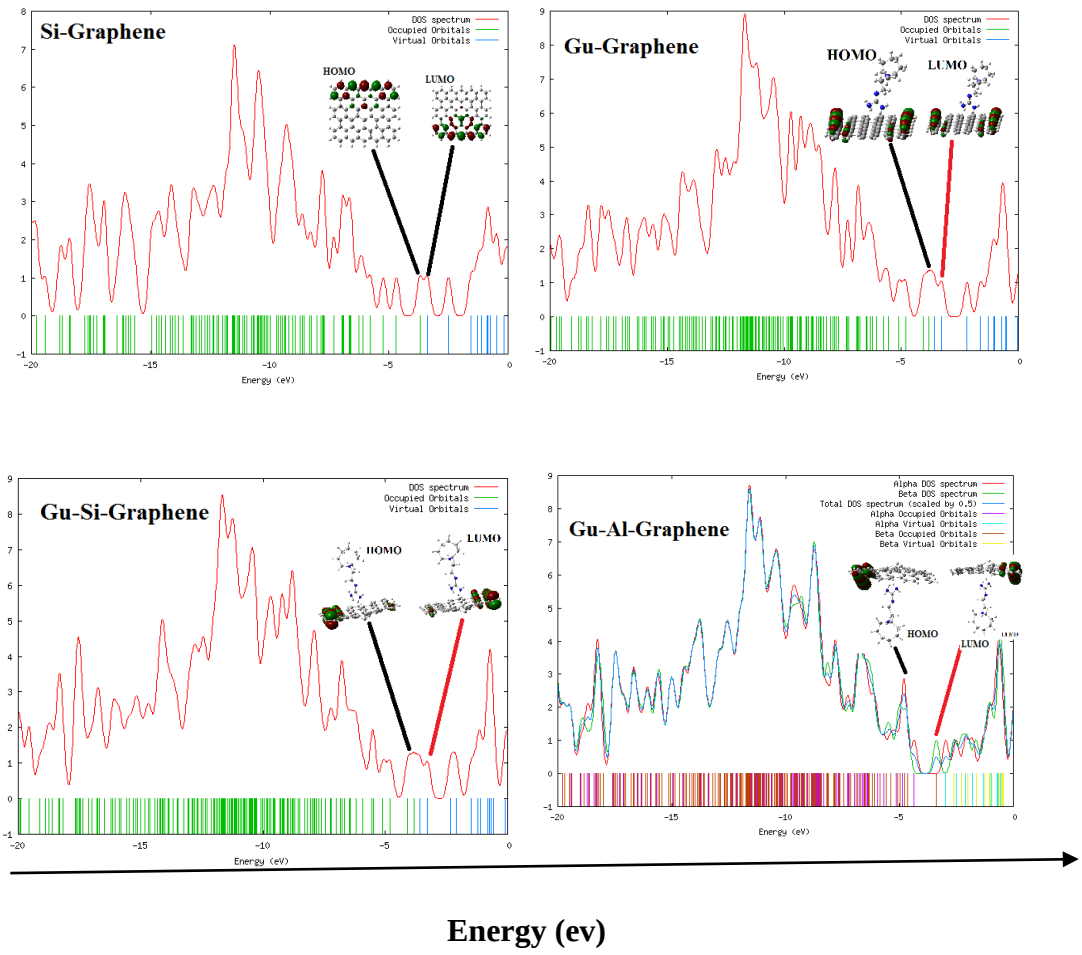

Figure 2. diagram of the density of state per energy for Al/ Si-graphene and Gu-Al/Si-graphene.

The distribution patterns of the frontier molecular orbital's; highest occupied molecular orbital's (HOMOs) and lowest unoccupied molecular orbital's (LUMOs) [39] were presented in Fig. 1 and Table 1. As Figure 1 indicates, the variance between HOMO and LUMO in Sun- Gr is -0.003 a.u which is less than other graphene derivatives in this study. The energy gaps in four modeled samples vary as below:

Egap(Al-gr) > Egap(Sun-Al-Gr) > Egap(Gr) > Egap(Si-Gr) > Egap(Sun-Si-Gr) > Egap(Sun-Gr)

As indicated energy gaps of all graphene derivatives follow the above trend. According to these results as the energy gap decreases, the electrical conductivity increases. Hence nano drug Sunitinib-graphene has the minimum energy gap while possessing maximum electrical conductivity.

Conclusion

In this study impacts of Sunitinib on graphene and Si-and Al doped graphene are surveyed. Based on the investigations it was revealed that due to the adsorption on graphene surface bond length and bond angles of doped atoms change when doped to Al and Si and the hybridation will change into sp3. Herein the adsorption is chemisorption and among all Sunitinib-graphene-Al has the maximum value. Dipole moment increases as a result of Sunitinib adsorption on graphene surface, hence the solubility of drug rises and it could be applied as a targeted drug. The comparison of calculated energy gap indicates that Sunitinib-graphene has the lowest energy gap and thus possesses the highest conductivity. In surveying nucleic magnetic resonance it can be conceived that in nano drug due to anisotropic effect graphene atoms bear more changes compared to graphene individually. Moreover, Nuclear Quadrupole Resonance (NQR) on graphene surface changes due to this adsorption.

Acknowledgment

The author is grateful to Pharmaceutical Sciences Branch, Islamic Azad University of Tehran for the support of this work.

References

[1] S. Benita, Microencapsulation Methods and Industrial Applications,USA, CRC Press, (2006).

[2] T. Y. Zakharian, A. Seryshev, B. Sitharaman, B. E. Gilbert, V. Knight and L. J. Wilson, *J. Am. Chem. Soc*., 127, 12508 (2005).

[3] C. Chen, G. Xing, J. Wang, Y. Zhao, B. Li, J. Tang, G. Jia, T. Wang, J. Sun, L. Xing, H. Yuan, Y. Gao, H. Meng, Z. Chen, F. Zhao, Z. Chai, X. Fang, *Nano Lett*., 5, 2050 (2005).

[4] X. Liang, H. Meng, Y. Wang, H. He, J. Meng, J. Lu, P. C. Wang, Y. Zhao, X. Gao, B. Sun, C. Chen, G. Xing, D. Shen, M. M. Gottesman, Y. Wu, J. Yin, L. Jia, *Proc. Natl. Acad. Sci*. *USA*, 107, 7449 (2010).

[5] Z. Liu, J. T. Robinson, S. M. Tabakman, K. Yang, H. Dai, *Materials Today*, 14, 316 (2011).

[6] J. Lee, K. Min, S. Hong, G. Kim, *Chemical Physics Letters*, 618, 57 (2015).

[7] A. Parga, F. Calleja, B. Borca, M. Passeggi, J. Hinarejos, F. Guinea, R. Miranda, *Phys. Rev. Lett.*, 100(5), 056807 (2008).

[8] W. Zhang, Z. Guo, D. Huang, Z. Liu, X. Guo, H. Zhong, *Biomaterials*, 32, 8555 (2011).

[9] A.P. Suryvanshi, M.F. Yu, J. Wen, C. Tang, Y. Bando, *Appl. Phys. Lett*., 84, 2527 (2004).

[10] Y. Chen, J. Zou, S.J. Campbell,G. Le, *Caer,Appl. Phys.Lett*., 84, 2430 (2004).

[11] G. Ciofani, V. Raffa, A. Menciassi, A. Cuschieri, *Nano Today*, 4, 8 (2009).

[12] G. Ciofani , S. Danti, S. Nitti, B. Mazzolaia, V. Mattolia, M. Giorgi, *International Journal of Pharmaceutics*, 444, 85 (2013).

[13] L. Fushen, W. Fei, C. Li. Kong, C. Yi, H. Xiaochun**,** *Nanosci. Nanotech. Lett*., 4, 949 (2012).

[14] X. Chen, P. Wu, M. Rousseas, D. Okawa, Z. Gartner, A. Zettl, C. R. Bertozzi, *J. Am. Chem. Soc*., 131, 890 (2009).

[15] S. D. Turcoa, G. Ciofanib, V. Cappelloc, M. Gemmic, T. Cervellia, C. Saponaroa, S. Nittid, B. Mazzolaib, G. Bastaa, V. Mattolib, *Colloids and Surfaces B, Biointerfaces.*, 111, 142 (2013).

[16] US Food and Drug Administration ,FDA approves new treatment for gastrointestinal and kidney cancer *(2006).*

[17] *J.T.* Hartmann, *L*. Kanz, *Arch Dermatol.*, 144 (11), 1525 (2008).

[18] J.Y. Blay, P. Reichardt, *Expert Rev Anticancer Ther*., 9 (6), 831 (2009).

[19] Z. Liu, S. Tabakman, K. Welsher, H. Dai, *Nano Res*., 2, 85 (2009).

[20] W. Yang, K. R. Ratinac, S. P. Ringer, P. Thordarson, J. J. Gooding, F. Braet, *Angew. Chem. Int. Ed*., 49, 2114 (2010).

[21] Z. Liu, K. Yang and S.T. Lee, *J. Mater. Chem*., 21, 586 (2011).

[22] W. Wu, S. Wieckowski, G. Pastorin, M. Benincasa, C. Klumpp, J. P. Briand, R. Gennaro, M. Prato, A. Bianco, *Angew. Chem. Int. Ed*., 44, 6358 (2005).

[23] G. Pastorin, W. Wu, S. Wieckowski, J.P. Briand, K.Kostarelos, M. Pratoand, A. Bianco, *Chem. Comm*., 1182 (2006).

[24] N. G. Sahoo, H. Bao, Y. Pan, M. Pal, M. Kakran, H. K. F. Cheng, L. Li, L. P. Tanb, *Chem. Commun*., 47, 5235 (2011).

[25] X. Chen, P. Wu, M. Rousseas, D. Okawa, Z. Gartner, A. Zettl, C. R. Bertozzi, *J. Am. Chem. Soc*., 131, 890 (2009).

[26] G. Ciofani , V. Raffa , A. Menciassi, A. Cuschieri, *Nanoscale Res Lett.,* 4, 113 (2009).

[27] X. Li, C.Zhi, N.Hanagata, M. Yamaguchi, Y. Bando, D.Golberg ,*Chem. Commun*., 49 7337 (2013).

[28] M. E. Khalifi, E. Duverger, T. Gharbi, H. Boulahdour, F. Picaud, *Phys. Chem. Chem. Phys*., 17, 30057 (2015).

[29] S. Mukhopadhyay, R. H. Scheicher, R. Pandey, S. P. Karna, *J. Phys. Chem. Lett*., 2, 2442 (2011).

[30] C. K. Yang, *Comp. Phys. Comm*., 182, 39 (2011).

[31] M. J. Frisch, G. W. Trucks, H. B. Schlegel, G. E. Scuseria, M. A. Robb, J. R. Cheeseman, J. A. Montgomery, T. Vreven, K. N. Kudin, J. C. Burant, J. M. Millam, S. S. Iyengar, J. Tomasi, V. Barone, B. Mennucci, M. Cossi, G. Scalmani, N. Rega, G. A. Petersson, H. Nakatsuji, M. Hada, M. Ehara, K. Toyota, R. Fukuda, J. Hasegawa, M. Ishida, T. Nakajima, Y. Honda, O. Kitao, H. Nakai, M. Klene, X. Li, J. E. Knox, H. P. Hratchian, J. B. Cross, V. Bakken, C. Adamo, J. Jaramillo, R. Gomperts, R. E. Stratmann, O. Yazyev, A. J. Austin, R. Cammi, C. Pomelli, J. W. Ochterski, P. Y. Ayala, K. Morokuma, G. A. Voth, P. Salvador, J. J. Dannenberg, V. G. Zakrzewski, S. Dapprich, A. D. Daniels, M. C. Strain, O. Farkas, D. K. Malick, A. D. Rabuck, K. Raghavachari, J. B. Foresman, J. V. Ortiz, Q. Cui, A. G. Baboul, S. Clifford, J. Cioslowski, B. B. Stefanov, G. Liu, A. Liashenko, P. Piskorz, I. Komaromi, R. L. Martin, D. J. Fox, T. Keith, Al M. A. Laham, C. Y. Peng, A. Nanayakkara, M. Challacombe, P. M. W. Gill, B. Johnson, W. Chen, M. W. Wong, C. Gonzalez, J. A. Pople, Revision2, Gaussian03, Gaussian Inc, Pittsburgh, PA (2003).

[32] R.S. Drago, Physical Methods for Chemists, second ed., Saunders College Publishing, New York (1992).

[33] M. Mirzaei, M. Yousefi, M. Meskinfam, *Solid State Sci*., 14 801 (2012).

[34] M. Mirzaei, N.L. Hadipour, *J. Comput. Chem*., 29, 832 (2008).

[35] a) A. Shameli, E. Balali, R. Khadivei, S. Shojaei, *Oriental Journal of chemistry*., 32(1), 291 (2016). b) F.S. Lavasani, A. Shameli, E. Balali, *Studia Universitatis Babes-Bolyai, Chemia.,* 62 (2017). c) S. Bagheri, A. Shameli, M. Darvishi, G. Fakhrpour, *Physica E, Low-dimensional Systems and Nanostructures*, *90*, 123 (2017).

[36] P. Pyykkö, *Mol Phys* ., 99, 1617 (2001).

[37] M. Mirzaei, *Journal of Molecular Modeling.*, 17, 89 (2010).

[38] V.A. Ferreira, H.W. LeiteAlves, *Journal of Crystal Growth..*, 310, 3973 (2008).

[39] A. Mokhtari, K. Harismah, M. Mirzaei, *Superlattices and Microstructures.*, 88, 56 (2015).